Vibration Mechanism Analysis of Magnetic Levitation Rotor System for Low Temperature Waste Heat Power Generation

Li JI [a], Jin ZHOU [b], HaiTong WU [b]

[a] HOHAI University, Nanjing 210098, China, @
[b] Nanjing University of Aeronautics and Astronautics, Nanjing, China, @

***Abstract*—By using high speed maglev generator, the efficiency of low temperature waste heat generation system can be improved significantly. In this paper, the unbalanced magnetic pull (UMP) in the maglev generator, caused by dynamic and static eccentricity, is calculated theoretically, and the analytical expression of the UMP is obtained based on Maxwell stress tensor method. Then, the vibration of a maglev rotor system under the action of the UMP and the mass unbalance force is analyzed by the numerical method. Lastly, the effects of different eccentricities, torque angles and loads on the rotor vibration are discussed in detail. The conclusions for the maglev rigid rotor system are useful for the future research.**

I. INTRODUCTION

The form of "turbine - reducer - generator" is commonly adopted by the traditional low-temperature waste heat power generation equipment, in which, the loss caused by the transmission and bearing system is up to 10% of the power of whole machine. Thus, these equipment have the disadvantages of low power generation efficiency, high cost, and large size, which limits their scale of development.

High-speed maglev turbine generator is developed by the reference of maglev aero-engine related technologies. The efficiency of it can be increased by 10% to 15% compared with traditional generator due to the removal of mechanical bearings, gearbox, and lubrication and oil supply system, which has great significance for the development of Chinese high-end manufacturing industry and low-carbon environmental protection policies [1-4].

However, the stiffness of magnetic bearings is much lower than that of general mechanical bearings [5]. There exists a great dynamic eccentricity when the rotor rotates, which will cause unbalanced magnetic pull (UMP) of motor, with the combined action of rotor mass unbalanced force and magnetic bearing control force, it can cause complex vibration of the generator rotor. In severe cases, the entire magnetic suspension system may be destabilized. Therefore, it is necessary to study the vibration mechanism of the maglev generator rotor.

The analysis of the vibration characteristics of eccentric rotor focus on conventional motors. The influence of static and dynamic eccentricity on the magnetic induction, output torque and loss of motor were presented in [6], and many valuable conclusions were obtained. According to the results of finite element analysis, the RBF neural network was used to establish the radial unbalanced force model in [7]. Considering both the static and dynamic eccentricity, the dynamic model of the permanent magnet motor rotor was established [8]. The unbalance response of the permanent magnet motor rotor was calculated based on FEM, and the vibration characteristics of the motor was analyzed [9]. The analytical model of the eccentric air gap magnetic field of a permanent magnet rotor was established by the regular perturbation theory, and the unbalanced tension under no-load condition was calculated [10]. However, there are few literatures about maglev motors. The vibration mechanism of maglev rigid rotor system was studied and its dynamic model was established, but the influence of the UMP was not taken into account [11]. The influence of UMP on the vibration of rotor and the stiffness of magnetic bearing was studied based on FEM, and many valuable conclusions were obtained. However, the conclusions were based on specific finite element model and the analytical model of the UMP was not obtained [12]. The radial magnetic force model of BSRM was established in consideration of magnetic saturation, but the effect of different eccentricity on the UMP and the vibration of rotor were not considered[13,14]. The radial force model of BSRM was established based on virtual displacement method, but the influence of rotor dynamic eccentricity is neglected in the derivation process [15].

In this paper, the analytical model of the UMP based on maglev generator is derived by the Maxwell stress tensor method and EMC. Combining with the unbalanced mass excitation of rotor and the control force of the magnetic bearings, the torque coupling and the vibration of rotor are studied. The conclusion obtained can provide theoretical support for suppressing the vibration of maglev generator.

II. MATHEMATICAL MODEL OF UMP OF PM MOTOR

Due to machining and assembly errors, the center of magnetic bearings stator, displacement sensor, catcher bearings [16], and motor stator are not in a straight line, while the rotor should suspend in the center of the catcher bearings according to the principle of magnetic

bearings, which causes the initial static eccentricity between the stator and rotor. Meanwhile, since the stiffness of magnetic bearing is relatively small, the rotor will rotate around one axis between its geometrical symmetry axis and the inertia spindle, and the dynamic eccentricity is generated. The schematic diagram of the rotor centroid cross section at this point is shown in Figure 1.

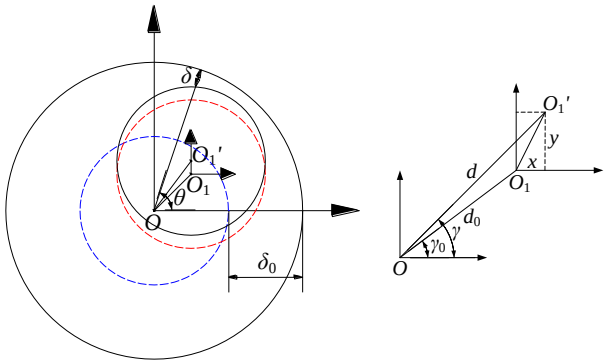

Figure 1. Cross-section of the maglev stator-rotor under air-gap eccentricity

Where O is the center of the motor stator, O_1 is the center of catcher bearing, O_1' is the geometric center of the rotor, δ_0 is the nominal air gap length, d_0 and γ_0 are the initial eccentricity and the eccentric angle under the static eccentricity; d and γ is actual eccentricity and eccentric angle of the rotor after taking the dynamic eccentricity into account; x and y are the offsets of the geometric center of the rotor from the horizontal and vertical direction of the maglev center. (It is assumed that the x direction is the same as the A axis of stator).

Since the rotor radius is much larger than the rotor center offset, the air gap length at any angle θ can be approximated as:

$$\delta(\theta) \approx \delta_0 - d\cos(\theta-\gamma) \tag{1}$$

Both the eccentricity and the eccentric angle in the equation can be expressed as a function of x and y.

$$d = \sqrt{(d_0\cos\gamma_0 + x)^2 + (d_0\sin\gamma_0 + y)^2} \tag{2}$$

$$\tan\gamma = \frac{d_0\sin\gamma_0 + y}{d_0\cos\gamma_0 + x} \tag{3}$$

The permeability at any air gap of motor can be expanded into a Fourier series form [17]:

$$\begin{aligned}\Lambda(\theta) &= \frac{\mu_0 \mathrm{d}S}{\delta(\theta)} = \frac{\mu_0 \mathrm{d}S}{\delta_0[1-\varepsilon\cos(\theta-\gamma)]} \\ &= \mathrm{d}S\sum_{n=0}^{\infty}\Lambda_n\cos n(\theta-\gamma)\end{aligned} \tag{4}$$

Where dS is the area of the magnetic pole area corresponding to the unit angle θ, ε is the relative eccentricity, and $\varepsilon=d/\delta_0$. The coefficient of Λ_n is shown in Appendix A.

According to the principle of the permanent magnet motor, the MMF of PM motor is composed of the permanent magnet equivalent MMF Fj and Armature MMF F_s under the condition of load. These two MMF remain synchronized at steady state and exhibit different phase differences under different control strategies. The resultant MMF in the air gap can be expressed as:

$$\begin{aligned}F(\theta) &= F_j(\theta) + F_s(\theta) \\ &= F_{j0}\cos(\alpha - p\theta) + F_{s0}\cos(\alpha - p\theta - \lambda)\end{aligned} \tag{5}$$

Where p is the rotor pole pair number; F_{j0} and F_{s0} represent the fundamental wave amplitudes of MMF of stator and rotor; α is the relative electrical angle between d-axis of the rotor and A-axis of the stator at any time. The frequency is equal to the frequency of the emitted current $\omega_e=p\omega_r$; λ is the angle between the MMF of stator and rotor (torque angle), which is related to the control strategy of motor.

Ignoring the magnetic potential of ferromagnetic materials, the expression of the magnetic induction intensity of the air gap at any angle θ based on EMC is:

$$\begin{aligned}B(\theta) &= \frac{\Lambda(\theta)\cdot F(\theta)}{S} \\ &= F(\theta)\cdot\sum_{n=0}^{\infty}\Lambda_n\cos n(\theta-\gamma)\end{aligned} \tag{6}$$

According to the basic formula of Maxwell stress method, the high-order term in the air gap permeability series is ignored, and only the first four items are retained in the calculation. In the case of one pole pair, the UMP in x and y direction of the rotor is shown in formula (7), where μ_0 is the vacuum permeability and k_n is the coefficient of UMP. See Appendix B for more details.

$$\begin{cases} f_{\mathrm{ump\_x}} = \dfrac{LR\pi}{8\mu_0}[k_1\cos\gamma + k_2\cos(\gamma+\lambda) \\ \quad + k_3\cos(\gamma-\lambda) + k_4\cos(2\alpha-\gamma) \\ \quad + k_5\cos(3\gamma-2\alpha) + k_6\cos(2\alpha-\gamma-\lambda) \\ \quad + k_7\cos(2\alpha-\gamma-2\lambda) + k_8\cos(3\gamma-2\alpha+2\lambda) \\ \quad + k_9\cos(3\gamma-2\alpha+\lambda)] \\ f_{\mathrm{ump\_y}} = \dfrac{LR\pi}{8\mu_0}[k_1\sin\gamma + k_2\sin(\gamma+\lambda) \\ \quad + k_3\sin(\gamma-\lambda) + k_4\sin(2\alpha-\gamma) \\ \quad + k_5\sin(3\gamma-2\alpha) + k_6\sin(2\alpha-\gamma-\lambda) \\ \quad + k_7\sin(2\alpha-\gamma-2\lambda) + k_8\sin(3\gamma-2\alpha+2\lambda) \\ \quad + k_9\sin(3\gamma-2\alpha+\lambda)] \end{cases} \tag{7}$$

Obviously, the UMP of rotor under load is very complicated. The static eccentricity of the conventional motor is dominant, thus, if the dynamic eccentricity is ignored (that is, d and γ are constant values), the UMP includes three fixed-direction force vectors, three double frequency positive sequence components and three double frequency negative sequence components. However, the dynamic eccentricity of maglev rotor cannot be ignored. The eccentric angle of the rotor is not fixed, but rotates at the same frequency as that of the rotational speed. Therefore, let $\alpha = \omega_r t$; $\gamma = \omega_r t + \varphi$. Assuming that the d-axis of rotor coincides with the A-axis of stator at initial position, φ represents the initial phase difference between the A-axis and the eccentric position. Bring it into formula (7), it is easy to find that all nine items of the UMP in the steady state are positive

sequence components with the same frequency as the speed. Therefore, the total UMP exhibits a rotational force vector with the same frequency and direction as the rotational speed, but the amplitude and phase of UMP are not determined, and depend on many factors such as the eccentricity, the torque angle (depending on the load and the motor control strategy), and the initial phase difference between the MMF and the eccentric angle.

It is necessary to simplify the formula (7), which is too complex and difficult to solve. In order to ensure the universality of the conclusions, qualitative analysis of each component in the formula is carried out. The magnitude of each component is analyzed under different eccentricity and load rates, and the curves obtained are shown in Figure 2.

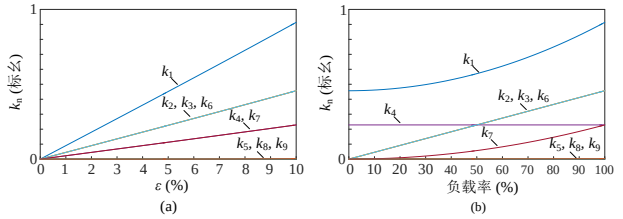

Figure 2. Unbalanced magnetic pull coefficient against eccentricity and load rate

It is obvious that the amplitudes of the coefficients k5, k8, and k9 within the entire load range and 10% eccentricity are extremely small, therefore, 5th, 8th, and 9th items in formula (7) are negligible The coefficients of the 2nd and 3rd items are the same and the phase is symmetric about γ. Thus, they can be merged into one force vector with the first items which is in the same direction as the eccentricity. The 4th, 6th, and 7th items are related to the unknown angle φ, so the synthesis can be seen as synchronous component, the direction of which is different from that of eccentricity, and the phase changes with the load and the eccentricity.

III. Dynamic Modeling of Maglev Rotor under UMP.

Figure 3 shows a simplified diagram of the rotor shaft system of a maglev generator. It consists of maglev rotor, generator stator, magnetic bearings, displacement sensor, and catcher bearing. Where A and B are the supporting positions of the radial magnetic bearings, x_A and x_B are the displacements corresponding to the radial magnetic bearings in the x direction, and O_C is the centroid of rotor. The spatial coordinate system and its positive direction are shown by the arrows in Figure 3.

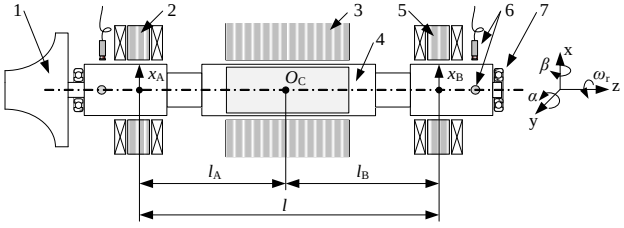

Figure 3. Schematic diagram of magnetic suspension rotor shafting

1. Turbine impeller; 2. Radial magnetic bearing A; 3. Generator stator; 4. Maglev rotor; 5. Radial magnetic bearing B; 6. Radial displacement sensor; 7. Catcher bearing

In the radial direction, the maglev rotor is subjected to a combination of unbalanced mass force, UMP, and control force of magnetic bearing. The control force f_{mb} of magnetic bearing near the working point can be regarded as a linear function of displacement and control current [4]:

$$f_{mb} = k_d \cdot d + k_i \cdot i \tag{8}$$

Where d is the eccentric displacement of rotor in a certain direction; i is the control current of the magnetic bearing; k_d is the displacement stiffness of the magnetic bearing and k_i is the current stiffness. The control current i is determined by the eccentric displacement and the specific control strategy. For the commonly used PID control strategy, the expression of i is as follows:

$$i = (-d) \cdot G_{PID} \cdot G_A \tag{9}$$

Where G_A is the transfer function of the power amplifier, which can be considered as a proportional component if the bandwidth of the power amplifier is large enough. The UMP of motor f_{ump} is shown in formula (7). The unbalance mass f_{ubm} on the x, y axis can be expressed as:

$$\begin{cases} f_{ubm\_x} = m(e_p - \Delta d)\omega_r^2 \cos(\omega_r t + \varphi) \\ f_{ubm\_y} = m(e_p - \Delta d)\omega_r^2 \sin(\omega_r t + \varphi) \end{cases} \tag{10}$$

Where e_p is the eccentricity of rotor (the distance from the center of mass to the centroid), $\Delta d = \sqrt{x^2 + y^2}$ is the distance from the centroid to the center of rotation, that is, the dynamic eccentricity, and φ is the phase of the unbalance mass. According to the formula (7~10) and the basic principle of rotor dynamics, the dynamic model of radial maglev rigid rotor system can be established as:

$$\boldsymbol{M\ddot{x}} + \boldsymbol{G\dot{x}} = \boldsymbol{K}_d \boldsymbol{x} + \boldsymbol{K}_i \boldsymbol{i} - \boldsymbol{E f}_{ub} \tag{11}$$

Where $x=[x_A, x_B, y_A, y_B]^T$ is the displacement of the maglev rotor relative to the equilibrium position of bearing A and B; i is the control current matrix of the magnetic bearings; f_{ub} represents the unbalanced excitation, mainly including the unbalance mass f_{ubm} and the unbalance magnetic pull f_{ump}; M is the generalized mass matrix; G is the gyro matrix; K_d is the displacement stiffness matrix; K_i is the current stiffness matrix; E is the unbalanced excitation response coefficient matrix, and the detailed expression is shown in Appendix C.

IV. Analysis of the Calculation Results

A. Analysis of the Calculation Results of UMP

In this paper, the UMP and its influence on the vibration of rotor are studied based on a 100kW high-speed maglev generator. The main parameters of the generator are shown in Table 1.

TABLE I. Parameters of the Maglev Generator

Parameters	value
Rotor quality	12.5 kg
Rotor equatorial inertial moment	0.2526 kg·m^2
Rotor polar inertial moment	0.0096 kg·m^2
air gap length	5 mm

Stator effective length	136 mm
Rotor diameter	56 mm
The length of the magnetic bearing A to the center of mass	101 mm
The length of the magnetic bearing B to the center of mass	199 mm

As shown in Figure 4, Figure 4(a) and (b) are the force conditions of the rotor under no static eccentricity and 0.1mm dynamic eccentricity. The four curves respectively represent the UMP of rotor in the x direction at four different initial dynamic eccentric angles, and the curves 1-4 correspond to the initial dynamic eccentric angles φ=0 °, 30 °, 60 °, and 90 °. In this case, the amplitude of the UMP is: 60.0N, 54.7N, 35.2N, 20.3N. It can be seen that under no-load conditions, the UMP depends not only on the eccentricity, but also on the angle between the eccentricity and the MMF. In the case of same dynamic eccentricity, if the direction of MMF is the same as the eccentricity (φ=0 °), the UMP of rotor is the maximum, and the phase of it is the same as that of dynamic eccentricity. If the direction of MMF is different from the eccentricity, the amplitude of UMP decreases and the phase shifts. The amplitude of UMP is the minimum when the direction of MMF is perpendicular to the eccentric direction (φ=90 °). Combining the UMP of x, y direction into one vector, as shown in Figure 4 (b). It can be seen that the UMP vector trajectory is circular only under dynamic eccentricity, and the amplitude of UMP in the x, y direction is always the same. The phase difference between the direction of MMF and eccentricity only affects the amplitude and phase of UMP without distorting the trajectory of the resultant force.

Figure4(c) and (d) show the UMP of rotor under both static eccentricity (magnitude 0.02mm) and dynamic eccentricity (magnitude 0.1mm). The curve 1-3 in the Figure correspond to the static eccentricity angles γ_0 =0 °, 45 °, and 90 ° respectively. In order to verify the effect of static eccentricity, setting the initial dynamic eccentricity angle φ = 0 °, the amplitude of UMP does not change much with the change of γ_0, but its waveform shows a direct current component. As shown in figure4(c), the mean value of curve 1-3 are 6.25N, 4.5N, and 3×10^{-15}N. It can be seen that when the static eccentricity is completely in x direction, the offset of F_x is maximum. When the static eccentricity is completely in y direction, the F_x is not affected, and the positive and negative half cycles are symmetrical, while the situation in the direction of y is opposite. It can be concluded that the static eccentricity will offset the UMP, and the direction of the offset is the same as that of static eccentricity.

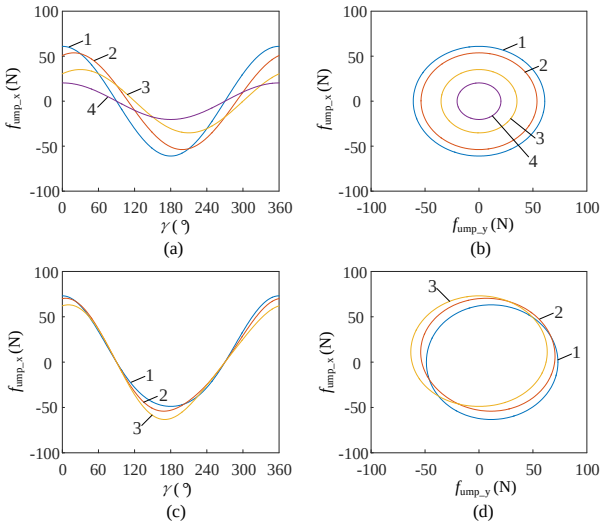

Figure 4. The waveforms of unbalanced magnetic pull under no-load

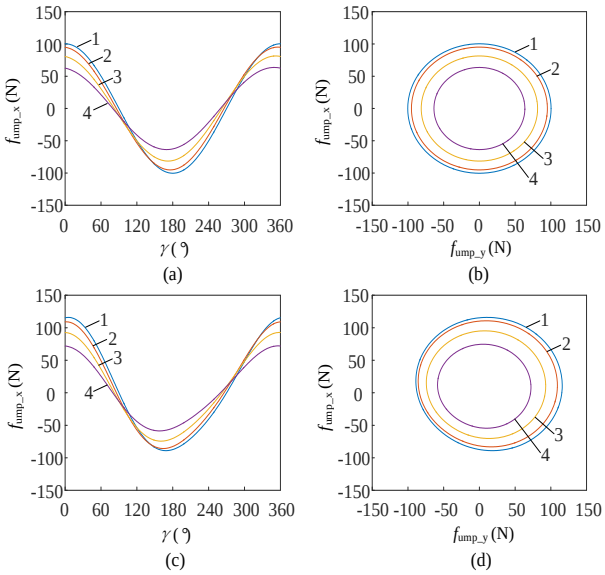

Figure 5. The waveforms of unbalanced magnetic pull during full-load

The force condition of the rotor under full-load is shown in Figure 5. Figure5 (a) and (b) show the UMP of rotor under dynamic eccentricity (0.1mm) and the initial phase difference angle φ= 0°. With the influence of different motor control strategies, the stator and rotor torque angle are different. In the paper, four conditions are studied. The curve 1-4 in the corresponding figure indicate the UMP in the x direction of rotor as the stator and rotor torque angle λ is 0°, 30°, 60°, and 90°, and the respective amplitudes are 100.3N, 95.1N, 81.4N and 63.6N. It can be seen that the change of torque angle affects both the amplitude and phase of UMP. The UMP of rotor is the maximum when the torque angle is zero. With the increase of the torque angle, the UMP is gradually reduced, and the phase is also changed. When the torque angle reaches 90 °, the UMP is minimum.

Figure5 (c) and (d) show the UMP of rotor under both static eccentricity (magnitude 0.02mm, static

eccentricity angle γ0=45°) and dynamic eccentricity (magnitude 0.1mm). As shown by these pictures that the UMP offsets in the positive direction of the x and y axes, and the change in its amplitude is the same as that in (a) (b). The UMP is the maximum when the torque angle is 0 °, and the minimum when the torque angle is 90 °.

The following conclusion can be obtained through the analysis of the UMP under no-load and full-load conditions: (1) The initial phase difference φ has great influence on the UMP, and when φ=0 °, the UMP is maximum, when φ=90 °, the UMP is minimum; (2) Static eccentricity has less influence on the UMP, but it produces DC component, and the magnitude of the DC component is proportional to that of static eccentricity, its direction is the same as that of static eccentricity; (3) The torque angle λ has a great influence on the UMP. When λ=0 °, the UMP is the maximum, and when the λ=90 °, the UMP is the minimum.

B. Analysis of the Vibration of Maglev Rotor

In section 2 of this paper, the dynamic model of the maglev rotor with unbalanced excitation is deduced as shown in formula (11), which satisfies the forced vibration form of the damping system under the harmonic force. Based on the maglev generator shown in Table 1, setting the speed to 9000r/min, the eccentricity of the rotor e_p = 10μm, and solve formula (11). The simulation results are shown in Figure 6.

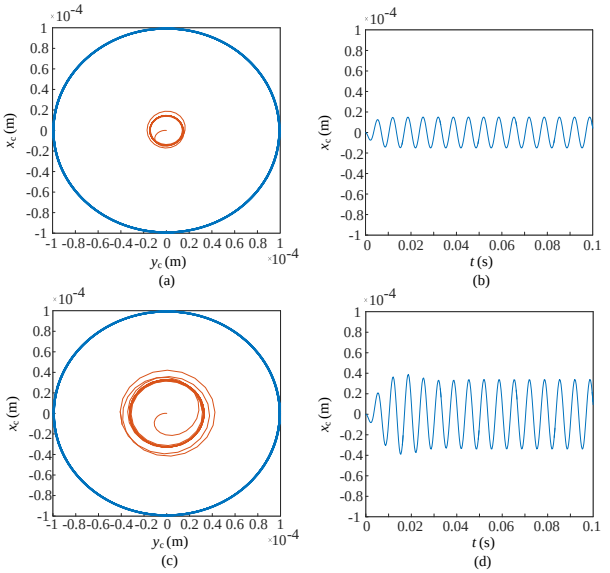

Figure 6. Simulation waveforms of rotor radial vibration with and without unbalanced magnetic pull

Figure 6 (a) and (b) are the axial trajectory and vibration waveform of the rotor in x direction only under the unbalance mass. The outer ring in Figure 6(a) represents the rotor's limit vibration range (0.1mm), beyond which the rotor will collide with the catcher bearing. It can be seen that under current rotation speed, if only the mass unbalance force is applied, the vibration of the rotor is small, and only 15μm after stabilization. Figure 6 (c) and (d) are the axial trajectory and vibration waveform of rotor in the x direction under both the mass unbalance force and UMP. It can be seen that the vibration increases significantly after taking the UMP into account, and reaches 34μm after stabilization, which is more than double the former. Therefore, the influence of UMP on the vibration of maglev rotor cannot be ignored.

V. TEST VERIFICATION

In order to verify the conclusion, experimental study of a 100kW maglev generator is carried out. The main parameters are shown in Table 1. Since the UMP is difficult to be test, the test mainly examines the influence of UMP on the suspension performance of the rotor at different torque angles. In the test, the speed of motor is raised to 4800 r/min. Meanwhile, the torque angle of the motor λ is adjusted through the vector control algorithm and the vibration of the rotor is observed, the results are shown in Figure 7.

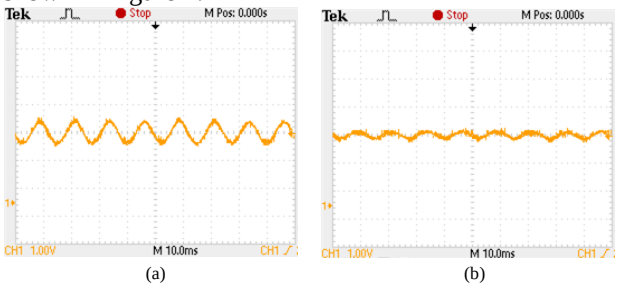

Figure 7. Experimental waveforms of rotor radial displacement under the different torque angle

Figure7 shows the radial vibration of the maglev rotor. The torque angle of the motor in 7 (a) is close to zero, and the armature current largely acts on the d-axis of the rotor. At this time, the frequency of the vibration signal detected by the radial displacement sensor is 80Hz, the peak value is 1.04V, and the measurement accuracy of the sensor is 20V/mm. At the current rotation speed, the rotor is subjected to forced vibration at the same frequency as the rotation speed under the combined action of the mass unbalance force and the UMP. The amplitude of the vibration is 26μm. At the same speed and the same bearing control parameters, the vector control algorithm of the frequency converter is adjusted to change the torque angle to 90 °. The vibration of the rotor is shown in Figure 7(b). At this time, the amplitude of the vibration is reduced to 12μm, which is only 46.15% of 7(a). Since the rotational speed and the control parameters of the magnetic bearing speed in these two tests are exactly the same, that is, the mass unbalanced force and the supporting characteristics in 7(a) and (b) are exactly the same. While the vibration of the rotor has changed greatly, which proves that the maglev rotor is actually affected by the UMP, and it is consistent with the theoretical analysis in Section 3. The smaller the torque angle, the greater the influence of unbalanced pull force. The smaller the torque angle, the greater the influence of UMP.

VI. CONCLUSION

In this paper, the UMP and the radial vibration of maglev rotor are studied based on the high-speed maglev generator. The analytical expression of the UMP is

derived based on the EMC and Maxwell stress tensor method. The main factors affecting the UMP are analyzed in detail through calculations, simulations and tests. The following conclusions can be drawn:

(1) In the maglev motor, where dynamic eccentricity is dominant, the UMP of the rotor appears as a rotational force vector with the same frequency and direction as that of rotation speed, and its amplitude and phase depend on the eccentricity, torque angle λ, and the initial phase difference φ between the MMF of rotor and the eccentric angle.

(2) Under no-load condition, the initial phase difference φ has a great influence on the UMP. With the same eccentricity, if $\varphi = 0°$, the UMP is maximum, and the phase of it is the same as that of the eccentricity. If $\varphi = 90°$, the UMP is minimum.

(3) Under load condition, the UMP is affected by the torque angle λ. With the same MMF of stator and rotor, if $\lambda = 0°$, the UMP is maximum. With the increase of λ, theUMP gradually decreases, and the phase also changes. If λ=90°, the UMP is minimum.

(4) Simulations and experiments prove that the UMP has great influence on the vibration of maglev rotor and cannot be ignored. While the UMP can be effectively reduced by adjusting the motor control strategy.

REFERENCES

[1] S. Rana, B. Orr, A. Iqbal, et al. Modelling and Optimization of Low-temperature Waste Heat Thermoelectric Generator System [J]. Energy Procedia, 2017, 110: 196-201.

[2] U. Chiarotti, V. Moroli, F. Menchetti, et al. Development of a Small Thermoelectric Generators Prototype for Energy Harvesting from Low Temperature Waste Heat at Industrial Plant [J]. Journal of Nanoscience & Nanotechnology, 2017, 17 (3): 1586-1591.

[3] Z. Wang, C. Cui. Design and Analysis on Low-temperature Waste Heat Power Generation Using Organic Rankine Cycle [J]. Power & Energy, 2013, 34(4): 321-324.

[4] L. Ji, L. Xu and C. Jin. Research on a Low Power Consumption Six-Pole Heteropolar Hybrid Magnetic Bearing [J]. IEEE Transactions on Magnetics, 2013, 49(8): 4918-4926.

[5] H. Gao, L. Xu. Real-time Feed-Forward Force Compen- sation for Active Magnetic Bearings System Based on H∞ Controller [J]. Chinese Journal of Mechanical Engineering, 2011, 24(1): 58-66.

[6] H. Kong, J. Liu. Study of rotor eccentricity effect on permanent magnet servo motor performance [J]. Electric Machines and Control 2016, 20(1): 52-59.

[7] J. Xiu, S. Wang. DSPM radial force static characteristic analysis and RBF NN modeling under rotor eccentric [C]. The 25th Chinese Control and Decision Conference (CCDC). 2013, Guiyang, China: 5174-5179.

[8] E. Yue, C. Gan, S. Yang. Vibration characteristics analysis of a rotor for a permanent magnet motor with Air-Gap Eccentricity [J]. JOURNAL OF VIBRATION AND SHOCK. 2014, 33(8): 29-34.

[9] X. Jiang, W. Li, Y. Chen, et al. Vibration characteristics research for the low speed direct drive high power PMSM [J]. Electric Machines and Control, 2017, 21(7): 73-77.

[10] C. Li, Y. Zhang, X. Zhou. Exact analytical solution of open-circuit air-gap magnetic field for slotted surface-mounted permanent-magnet motors with rotor eccentricity [J]. Electric Machines and Control, 2014, 18(10): 27-35.

[11] J. Fang, H. Zhang, H. Liu. Vibration mechanism analysis and dynamic model development of magnetically suspended rigid rotor system [J]. Control Theory & Applications. 2014, 31(12): 1707-1713.

[12] B. Han, S. Zheng, X. Liu. Unbalanced Magnetic Pull Effect on Stiffness Models of Active Magnetic Bearing due to Rotor Eccentricity in Brushless DC Motor Using Finite Element Method [J]. Mathematical Problems in Engineering. 2013: 1-10.

[13] Y. Yang, Z. Deng, X. Cao, et al. Magnetic radial force model of bearingless switched reluctance motor [J]. Electric Machines and Control 2009, 13(3): 376-382.

[14] X. Cao, Z. Deng, G. Yang, et al. Mathematical Model of Bearingless Switched Reluctance Motors Based on Maxwell Stress Tensor Method [J]. Proceedings of the CSEE. 2009, 29 (3): 78-83.

[15] X. Sun, L. Chen, Z. Yang, et al. Modeling of a Bearingless Permanent Magnet Synchronous Motor Considering Rotor Eccentricity and Coupling Relationship of Windings[J]. Transactions of China Electrotechnical Society, 2013, 28(3): 63-70.

[16] Y. Zhu, C. Jin, L. Xu. Dynamic response of rotor drops onto double-decker catcher bearing [J], Chinese Journal of Mechanical Engineering. 2013, 26 (1): 104-113.

[17] D. Guo, F. Chu and D. Chen. The Unbalanced Magnetic Pull and Its Effects on Vibration in A Three-Phase Generator with Eccentric Rotor [J]. Journal of Sound and Vibration, 2002, 254(2): 297-312.

Appendix A:

The permeability at any air gap of the motor can be expanded into Fourier series.

$$\Lambda(\theta)=\frac{\mu_0 \mathrm{d}S}{\delta(\theta)}=\frac{\mu_0 \mathrm{d}S}{\delta_0[1-\varepsilon\cos(\theta-\gamma)]}=\mathrm{d}S\sum_{n=0}^{\infty}\Lambda_n\cos n(\theta-\gamma) \tag{1}$$

Where dS is the area of the magnetic pole area corresponding to the unit angle θ, ε is the relative eccentricity, and $\varepsilon=d/\delta_0$. The coefficient of Λ_n is shown in formula2.

$$\Lambda_n=\begin{cases}\dfrac{\mu_0}{\delta_0\sqrt{1-\varepsilon^2}} & (n=0)\\ \dfrac{2\mu_0}{\delta_0\sqrt{1-\varepsilon^2}}\left(\dfrac{1-\sqrt{1-\varepsilon^2}}{\varepsilon}\right)^n & (n>0)\end{cases} \tag{2}$$

Appendix B:

The UMP of the rotor in the x and y directions is shown in formula (1), where μ_0 is the vacuum permeability and k_n is the coefficient of UMP.

$$\begin{cases} f_{\mathrm{ump\_x}}=\dfrac{LR\pi}{8\mu_0}[k_1\cos\gamma+k_2\cos(\gamma+\lambda)\\ \quad +k_3\cos(\gamma-\lambda)+k_4\cos(2\alpha-\gamma)\\ \quad +k_5\cos(3\gamma-2\alpha)+k_6\cos(2\alpha-\gamma-\lambda)\\ \quad +k_7\cos(2\alpha-\gamma-2\lambda)+k_8\cos(3\gamma-2\alpha+2\lambda)\\ \quad +k_9\cos(3\gamma-2\alpha+\lambda)]\\ f_{\mathrm{ump\_y}}=\dfrac{LR\pi}{8\mu_0}[k_1\sin\gamma+k_2\sin(\gamma+\lambda)\\ \quad +k_3\sin(\gamma-\lambda)+k_4\sin(2\alpha-\gamma)\\ \quad +k_5\sin(3\gamma-2\alpha)+k_6\sin(2\alpha-\gamma-\lambda)\\ \quad +k_7\sin(2\alpha-\gamma-2\lambda)+k_8\sin(3\gamma-2\alpha+2\lambda)\\ \quad +k_9\sin(3\gamma-2\alpha+\lambda)]\end{cases} \tag{1}$$

$$\begin{aligned}
k_1&=4F_{\mathrm{j0}}^2\Lambda_0\Lambda_1+2F_{\mathrm{j0}}^2\Lambda_1\Lambda_2+2F_{\mathrm{j0}}^2\Lambda_2\Lambda_3+4F_{\mathrm{s0}}^2\Lambda_0\Lambda_1+2F_{\mathrm{s0}}^2\Lambda_1\Lambda_2+2F_{\mathrm{s0}}^2\Lambda_2\Lambda_3\\
k_2&=4F_{\mathrm{j0}}F_{\mathrm{s0}}\Lambda_0\Lambda_1+2F_{\mathrm{j0}}F_{\mathrm{s0}}\Lambda_1\Lambda_2+2F_{\mathrm{j0}}F_{\mathrm{s0}}\Lambda_2\Lambda_3\\
k_3&=4F_{\mathrm{j0}}F_{\mathrm{s0}}\Lambda_0\Lambda_1+2F_{\mathrm{j0}}F_{\mathrm{s0}}\Lambda_1\Lambda_2+2F_{\mathrm{j0}}F_{\mathrm{s0}}\Lambda_2\Lambda_3\\
k_4&=2F_{\mathrm{j0}}^2\Lambda_0\Lambda_1+F_{\mathrm{j0}}^2\Lambda_1\Lambda_2+F_{\mathrm{j0}}^2\Lambda_2\Lambda_3\\
k_5&=2F_{\mathrm{j0}}^2\Lambda_0\Lambda_3+F_{\mathrm{j0}}^2\Lambda_1\Lambda_2\\
k_6&=4F_{\mathrm{j0}}F_{\mathrm{s0}}\Lambda_0\Lambda_1+2F_{\mathrm{j0}}F_{\mathrm{s0}}\Lambda_1\Lambda_2+2F_{\mathrm{j0}}F_{\mathrm{s0}}\Lambda_2\Lambda_3\\
k_7&=2F_{\mathrm{s0}}^2\Lambda_0\Lambda_1+F_{\mathrm{s0}}^2\Lambda_1\Lambda_2+F_{\mathrm{s0}}^2\Lambda_2\Lambda_3\\
k_8&=2F_{\mathrm{s0}}^2\Lambda_0\Lambda_3+F_{\mathrm{s0}}^2\Lambda_1\Lambda_2\\
k_9&=4F_{\mathrm{j0}}F_{\mathrm{s0}}\Lambda_0\Lambda_3+2F_{\mathrm{j0}}F_{\mathrm{s0}}\Lambda_1\Lambda_2
\end{aligned} \tag{2}$$

Appendix C:

According to the basic principles of rotor dynamics, the dynamic model of radial magnetic suspension rigid rotor system is established:

$$\boldsymbol{M}\ddot{\boldsymbol{x}}+\boldsymbol{G}\dot{\boldsymbol{x}}=\boldsymbol{K}_{\mathrm{d}}\boldsymbol{x}+\boldsymbol{K}_{\mathrm{i}}\boldsymbol{i}-\boldsymbol{E}\boldsymbol{f}_{\mathrm{ub}} \tag{1}$$

Where $x=[x_{\mathrm{A}}, x_{\mathrm{B}}, y_{\mathrm{A}}, y_{\mathrm{B}}]^{\mathrm{T}}$ is the displacement of the maglev rotor relative to the equilibrium position at bearing A and B; i is the control current matrix of the magnetic bearings; f_{ub} represents the unbalanced excitation, mainly including the unbalance mass f_{ubm} and the unbalance magnetic pull f_{ump}; M is the generalized mass matrix; G is the gyro matrix; K_{d} is the displacement stiffness matrix; K_{i} is the current stiffness matrix; E is the unbalanced excitation response coefficient matrix, and the detailed expression is shown below:

$$\begin{bmatrix} \frac{ml_{\mathrm{B}}^2+J_{\mathrm{d}}}{(l_{\mathrm{A}}+l_{\mathrm{B}})^2} & \frac{ml_{\mathrm{A}}l_{\mathrm{B}}-J_{\mathrm{d}}}{(l_{\mathrm{A}}+l_{\mathrm{B}})^2} & 0 & 0 \\ \frac{ml_{\mathrm{A}}l_{\mathrm{B}}-J_{\mathrm{d}}}{(l_{\mathrm{A}}+l_{\mathrm{B}})^2} & \frac{ml_{\mathrm{A}}^2+J_{\mathrm{d}}}{(l_{\mathrm{A}}+l_{\mathrm{B}})^2} & 0 & 0 \\ 0 & 0 & \frac{ml_{\mathrm{B}}^2+J_{\mathrm{d}}}{(l_{\mathrm{A}}+l_{\mathrm{B}})^2} & \frac{ml_{\mathrm{A}}l_{\mathrm{B}}-J_{\mathrm{d}}}{(l_{\mathrm{A}}+l_{\mathrm{B}})^2} \\ 0 & 0 & \frac{ml_{\mathrm{A}}l_{\mathrm{B}}-J_{\mathrm{d}}}{(l_{\mathrm{A}}+l_{\mathrm{B}})^2} & \frac{ml_{\mathrm{A}}^2+J_{\mathrm{d}}}{(l_{\mathrm{A}}+l_{\mathrm{B}})^2} \end{bmatrix} \begin{bmatrix} \ddot{x}_{\mathrm{A}} \\ \ddot{x}_{\mathrm{B}} \\ \ddot{y}_{\mathrm{A}} \\ \ddot{y}_{\mathrm{B}} \end{bmatrix} + \begin{bmatrix} 0 & 0 & \frac{\omega_{\mathrm{r}}J_{\mathrm{p}}}{(l_{\mathrm{A}}+l_{\mathrm{B}})^2} & -\frac{\omega_{\mathrm{r}}J_{\mathrm{p}}}{(l_{\mathrm{A}}+l_{\mathrm{B}})^2} \\ 0 & 0 & -\frac{\omega_{\mathrm{r}}J_{\mathrm{p}}}{(l_{\mathrm{A}}+l_{\mathrm{B}})^2} & \frac{\omega_{\mathrm{r}}J_{\mathrm{p}}}{(l_{\mathrm{A}}+l_{\mathrm{B}})^2} \\ -\frac{\omega_{\mathrm{r}}J_{\mathrm{p}}}{(l_{\mathrm{A}}+l_{\mathrm{B}})^2} & \frac{\omega_{\mathrm{r}}J_{\mathrm{p}}}{(l_{\mathrm{A}}+l_{\mathrm{B}})^2} & 0 & 0 \\ \frac{\omega_{\mathrm{r}}J_{\mathrm{p}}}{(l_{\mathrm{A}}+l_{\mathrm{B}})^2} & -\frac{\omega_{\mathrm{r}}J_{\mathrm{p}}}{(l_{\mathrm{A}}+l_{\mathrm{B}})^2} & 0 & 0 \end{bmatrix} \begin{bmatrix} \dot{x}_{\mathrm{A}} \\ \dot{x}_{\mathrm{B}} \\ \dot{y}_{\mathrm{A}} \\ \dot{y}_{\mathrm{B}} \end{bmatrix} - \begin{bmatrix} k_{\mathrm{xy1}} & 0 & 0 & 0 \\ 0 & k_{\mathrm{xy2}} & 0 & 0 \\ 0 & 0 & k_{\mathrm{xy3}} & 0 \\ 0 & 0 & 0 & k_{\mathrm{xy4}} \end{bmatrix} \begin{bmatrix} x_{\mathrm{A}} \\ x_{\mathrm{B}} \\ y_{\mathrm{A}} \\ y_{\mathrm{B}} \end{bmatrix} - \begin{bmatrix} k_{\mathrm{i1}} & 0 & 0 & 0 \\ 0 & k_{\mathrm{i2}} & 0 & 0 \\ 0 & 0 & k_{\mathrm{i3}} & 0 \\ 0 & 0 & 0 & k_{\mathrm{i4}} \end{bmatrix} \begin{bmatrix} i_{\mathrm{xA}} \\ i_{\mathrm{xB}} \\ i_{\mathrm{yA}} \\ i_{\mathrm{yB}} \end{bmatrix} + \begin{bmatrix} \frac{l_{\mathrm{B}}}{l_{\mathrm{A}}+l_{\mathrm{B}}} & 0 & 0 & 0 \\ \frac{l_{\mathrm{A}}}{l_{\mathrm{A}}+l_{\mathrm{B}}} & 0 & 0 & 0 \\ 0 & 0 & \frac{l_{\mathrm{B}}}{l_{\mathrm{A}}+l_{\mathrm{B}}} & 0 \\ 0 & 0 & \frac{l_{\mathrm{A}}}{l_{\mathrm{A}}+l_{\mathrm{B}}} & 0 \end{bmatrix} \begin{bmatrix} f_{\mathrm{ub\_x}} \\ 0 \\ f_{\mathrm{ub\_y}} \\ 0 \end{bmatrix} = 0 \tag{2}$$